

Agglomeration Characteristics of Sludge Combustion in a Bench-Scale Fluidized Bed Combustor

Jingai Shao,^{†,‡} Dong Ho Lee,[‡] Rong Yan,^{*,‡} Ming Liu,[‡] Xiaoling Wang,[‡] David Tee Liang,[‡] Timothy John White,[§] and Hanping Chen[†]

State Key Laboratory of Coal Combustion, Huazhong University of Science and Technology, Wuhan, 430074, P. R. China, Institute of Environmental Science and Engineering, Nanyang Technological University, Innovation Center, Block 2, Unit 237, 18 Nanyang Drive, Singapore 637723, and School of Materials Science and Engineering, Nanyang Technological University, Block N4.1, Nanyang Avenue, Singapore 639798

Received January 2, 2007. Revised Manuscript Received May 29, 2007

In this study, sludge combustion was carried out in a bench-scale fluidized bed combustor to investigate the formation of agglomerates, followed by a thorough identification of bed materials and agglomerates using scanning electron microscopy/energy-dispersive X-ray spectrometry (SEM/EDX), X-ray diffraction (XRD), and X-ray fluorescence (XRF). Agglomeration invariably became more severe at higher temperatures with degraded sand as the bed material compared to fresh sand. Two major crystalline components, hematite (Fe₂O₃) and quartz (SiO₂), were detected in agglomerates, showing that the eutectics of iron and silicate with the viscous phase might be one of the promoters of bed agglomeration. SEM/EDX analysis revealed the agglomeration progress, suggesting the role of Si (from sand particles) and P, Mg, and Ca (from sludge) in initializing the formation of sticky surface of sand particles to act as a glue matter, followed by the formation of an agglomerate bridge contributed most likely by Fe, then by Al, K, and Na. The bed agglomeration observed was possibly attributed to both melt-induced and coating-induced mechanisms. Furthermore, the behavior of mineral matters in sludge combustion was simulated by means of thermodynamic multiphase multicomponent equilibrium (TPCE) calculations. The thermodynamically major low melting point species formed in sludge combustion were predicted. In combining the experimental and computational results, it is believed that alkali phosphates (KPO₃ and NaPO₃) and the eutectics of Fe₂O₃ and SiO₂ might play the most important role in bed agglomeration, by forming low melting point compounds, in the course of sludge combustion.

Introduction

Increasing quantities of sewage sludge arising from the proliferation of urban wastewater plants has generated concern regarding its disposal and reuse in many countries.^{1–4} Sludge incineration is considered an attractive alternative, which offers several advantages including large volume reductions (90%) to a stabilized ash, the thermal destruction of pathogens and toxic compounds, and the recovery of energy potential, with the calorific value of dry sludge being similar to that of lignite.² Fluidized bed combustion (FBC) is a flexible incineration technology for sludge treatment because the boiler design allows combustion and energy recovery from mixtures of low-grade fuels.⁵ However, FBC is sensitive to ash transformation properties and mineralogy during incineration.

Ash related problems include fusion and crystallization to form slag deposits, vaporization and condensation associated with fouling of furnace systems, corrosive interaction with internal boiler components, abrasion by mineral particles, and agglomeration and sintering that all contribute to defluidization.^{5,6} Bed agglomeration, which depends on geometry, process conditions, ash chemistry, and ash-bed material interactions,^{7,8} is of particular concern as it often leads to costly and unscheduled shutdowns of heat and power boilers.^{7–11} Although many reports regarding the agglomeration issue are available in the literature, a precise and quantitative knowledge of the bed agglomeration process during fluidized bed combustion of biomass fuels, especially sewage sludge, has not yet been clarified.

The effects of various factors on bed agglomeration were previously investigated, including fuel properties, temperature, fuel blending ratio, gas velocity, particle size, combustion

* To whom correspondence should be addressed. Telephone: 65-67943244. Fax: 65-67921291. E-mail: ryan@ntu.edu.sg.

[†] Huazhong University of Science and Technology.

[‡] Institute of Environmental Science and Engineering, Nanyang Technological University.

[§] School of Materials Science and Engineering, Nanyang Technological University.

(1) Rio, S.; Faur-Brasquet, C.; LeCoq, L.; LeCloirec, P. *Environ. Sci. Technol.* **2005**, *39*, 4249–4257.

(2) Hartman, M.; Svoboda, K.; Pohorely, M.; Trnka, O. *Ind. Eng. Chem. Res.* **2005**, *44*, 3432–3441.

(3) Yao, H.; Naruse, I. *Energy Fuels* **2005**, *19*, 2298–2303.

(4) Francisca Gomez-Rico, M.; Font, R.; Fullana, A.; Martin-Gullon, I. *J. Anal. Appl. Pyrolysis* **2005**, *74*, 421–428.

(5) Yan, R.; Liang, D. T.; Laursen, K.; Li, Y.; Tsen, L.; Tay, J. H. *Fuel* **2003**, *82*, 843–851.

(6) Ward, C. R. *Int. J. Coal Geol.* **2002**, *50*, 135–168.

(7) Zevenhoven-Onderwater, M.; Backman, R.; Skrifvars, B. J.; Hupa, M. *Fuel* **2001**, *80*, 1489–1502.

(8) Tiainen, M.; Daavitsainen, J.; Laitinen, R. S. *Energy Fuels* **2002**, *16*, 871–877.

(9) Zevenhoven-Onderwater, M.; Blomquist, J. P.; Skrifvars, B. J.; Backman, R.; Hupa, M. *Fuel* **2000**, *79*, 1353–1361.

(10) Zevenhoven-Onderwater, M.; Backman, R.; Skrifvars, B. J.; Hupa, M.; Liliendahl, T.; Rosen, C.; Sjoström, K.; Engvall, K.; Hallgren, A. *Fuel* **2001**, *80*, 1503–1512.

(11) Theis, M.; Skrifvars, B. J.; Zevenhoven, M.; Hupa, M.; Tran, H. *Fuel* **2006**, *85*, 1992–2001.

Table 1. Properties of Sewage Sludge Samples^a

sample	proximate analysis (wt %)				ultimate analysis (wt %) ^b					LHV (MJ/kg) ^b
	M _{ad}	V _{ad}	FC _{ad}	A _{ad}	N	C	H	S	O	
S1	59.63	31.89	0.12	8.36	3.63	39.17	7.5	1.29	48.41	17.75
S2	70.14	19.22	0	10.69	2.72	37.53	6.3	0.98	52.47	16.59
S3	60.01	32.91	0.93	6.15	3.69	39.55	7.75	1.27	47.74	16.2
S4	63.36	28.82	0	7.85	4.27	44.03	8.4	1.45	41.85	16.96

^a M, moisture content; V, volatile matters; A, ash; FC, fixed carbon; ad, on air-dried basis; LHV, lower heating value. The O content was determined by difference. ^b Determined on a dry basis.

stoichiometry, ash composition, and static bed height.^{5,7,12–14} Yan et al.⁵ found that fuels with high content of V, S, Na, and Cl elements might cause bed agglomeration and an optimal blending ratio of fuels would help in reducing the sintering. Lin et al.¹² reported that agglomeration was accelerated by temperature increases, while defluidization time was prolonged as the gas velocity increases and sand particle size decreases. It was also found that high gas velocity delayed agglomeration, but a higher static bed height facilitated agglomeration.¹³

Ash chemistry plays an important role in bed agglomeration, as fuels contain variable amounts of alkalis (e.g., K, Na), alkali earths (e.g., Ca, Mg), silicon (Si), iron (Fe), sulfur (S), vanadium (V), and chlorine (Cl) bearing compounds^{5,8,15,16} that might form low-temperature eutectics leading to incipient surface melts and finally defluidization. However, the relationship between bed agglomeration and fuel chemistry is very complex. Yan et al.⁵ reported that Al₂(SO₄)₃, Fe₂(SO₄)₃, Na₂SO₄, NaCl, Na₂SiO₃, and V₂O₅ could be the main agglomeration promoters in the multifuel combustion system. Tiainen et al.⁸ indicated that ion-rich coated quartz particles resulted in severely agglomerating in peat ash and the scanning electron microscopy/energy-dispersive X-ray spectrometry (SEM/EDX) result confirmed the formation of a wide range of iron aluminosilicates that further explained the formation of low melting point compounds. Lin et al.¹² found that Al₂(SO₄)₃, CaO, K₂O, MgO, Na₂O, and P₂O₅ were primarily responsible for the formation of liquid bridges, which enhanced sintering and agglomeration of particles. Elsewhere, Nielsen et al.¹⁷ indicated that, KCl, K₂SO₄, and Fe_xO_y might lead to the formation of a melted layer in a straw-fired boiler.

The possible mechanisms associated were proposed: “melt-induced” and “coating-introduced” agglomeration were the two main routes.^{18–20} For the former case, bed materials were directly glued together by a separated ash-derived melt phase, while, for the latter case, a coating layer was formed on the bed particles followed by subsequent adhesion and agglomeration. It was reported that coating layers formed on the bed particles were considered to be more common.^{18,20} Brus et al.¹⁹ found that coating-induced agglomeration with subsequent attack (reaction) and diffusion by calcium into the quartz bed material to be the dominating bed agglomeration mechanism for wood fuels. Nevertheless, the mechanism of bed agglomeration has not been fully understood, and further investigations are thus necessary.

The characteristics of agglomerates formed in sewage sludge combustion have seldom been examined. In this study, the chemistry of ash generated during sludge combustion was investigated using a bench-scale fluidized bed combustor to better understand the agglomeration characteristics, particularly with respect to fuel composition, ash components, bed material, and temperature. The bed agglomeration mechanism for sludge was proposed. The experimental identification of agglomeration promoters was supplemented with thermodynamic multiphase multicomponent equilibrium (TPCE) analysis.

Experimental Section

Sample Preparation and Characterization. Four sewage sludge samples (S1–S4) were investigated in this study. Prior to combustion, the samples were oven dried (Contherm Thermotec 2000) at 105 °C for ~16 h to remove moisture. The dried sludge samples were ground to less than 0.1 mm for further characterization. Proximate analyses of sludge samples were conducted using ASTM standards to obtain moisture content, volatiles, fixed carbon, and ash content.²¹ Ultimate analyses of the dried samples for carbon, hydrogen, nitrogen, and sulfur were carried out with a CHNS/O elementary analyzer (Perkin-Elmer 2400 series II). The calorimetric values of the dried sludge samples were measured by bomb calorimetry (Parr 1260). The results are shown in Table 1. All the materials possessed high moisture content (M) > 60 wt %, a medium volatile content (V) of ~20 to 30 wt %, and minor fixed carbon (FC) < 1 wt %. The oxygen content of sludge was relatively high, while combustible nitrogen and sulfur exceeded other types of biomass, such as rice straw and wood. It was suggested that extra flue gas treatment equipment might be needed during combustion. The heating values ranging from 16.2 to 17.59 MJ/kg indicated that incineration could be a feasible option to treat those sludge samples.

Before conducting a combustion test in the FB reactor, the ash fusion temperature of sludge was measured using thermogravimetric analyzer and differential scanning calorimetry (TGA/DSC; NETZSCH, STA 409C, Germany). The operating parameters were set as balance gas (N₂) 75 mL/min and sample gas (air) 50 mL/min, heating rate 30 °C/min, start temperature 25 °C, and end temperature 1300 °C. For each run, ~15 mg of ashed sludge sample (treated by low-temperature ashing at 450 °C for 15 h) was used. According to the literature,²² the onset of fusion phenomenon of a powder can be sensitively detected using DSC or differential thermal analysis (DTA) techniques when the DSC/DTA line shift becomes progressively larger and reaches a steady state. In this study, the onset fusion temperature was selected where the DSC/DTA plot started a largely endothermic line shift while the TG plot shift remained gradual. The detected ash fusion temperatures of S1–S4 were 1120, 1055, 1096, and 1067 °C, respectively.

Experimental Setup and Procedures. The bench-scale fluidized bed unit was constructed from a quartz tube of inner diameter of

(12) Lin, W.; Dam-Johansen, K.; Frandsen, F. *Chem. Eng. J.* **2003**, *96*, 171–185.

(13) Lin, C. L.; Wey, M. Y. *Fuel* **2004**, *83*, 2335–2343.

(14) Skrifvars, B. J.; Backman, R.; Hupa, M. *Fuel Process. Technol.* **1998**, *56*, 55–67.

(15) Ohman, M.; Nordin, A. *Energy Fuels* **1998**, *12*, 90–94.

(16) Arvelakis, S.; Gehrmann, H.; Beckmann, M.; Koukios, E. G. *Fuel* **2003**, *82*, 1261–1270.

(17) Nielsen, H. P.; Frandsen, F. J.; Dam-Johansen, K. *Energy Fuels* **1999**, *13*, 1114–1121.

(18) Ohman, M.; Pommer, L.; Nordin, A. *Energy Fuels* **2005**, *19*, 1742–1748.

(19) Brus, E.; Ohman, M.; Nordin, A. *Energy Fuels* **2005**, *19*, 825–832.

(20) Nuutinen, L. H.; Tiainen, M. S.; Virtanen, M. E.; Enestam, S. H.; Laitinen, R. S. *Energy Fuels* **2004**, *18*, 127–139.

(21) Mayoral, M. C.; Izquierdo, M. T.; Andres, J. M.; Rubio, B. *Thermochim. Acta* **2001**, *370*, 91–97.

(22) Chaklader, A. C. D.; Warren, I. H.; Lau, M. *Mineral Matter Content and Gross Properties of Hat Creek Coal*; The University of British Columbia, Department of Metallurgy: Vancouver, Canada, Jan–Mar 1977.

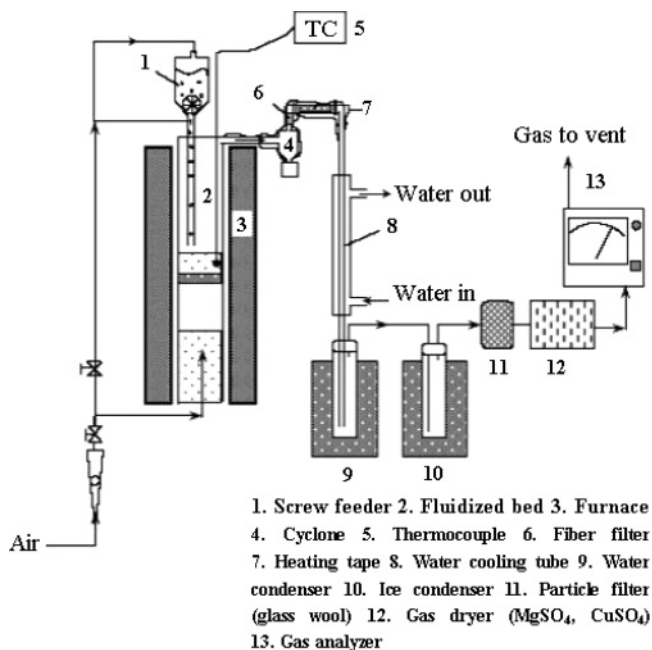


Figure 1. Schematic of bench-scale fluidized bed reactor.

50 mm and total height of 410 mm (Figure 1). The bed was filled with quartz sand (melting temperature 1450 °C) of ~0.3 mm to a height of approximately 100 mm. The perforated gas distributor was covered by a thin layer of quartz wool to contain the sand, and above which was packed a layer of quartz beads (~3 mm in diameter) to enhance the gas distribution.

To form and maintain a stable fluidization, the minimum and terminal velocities of gas flow and pressure drop of the bed were determined theoretically and confirmed by experimental pretrials. Other critical operating parameters considered included temperature, residence time (RT), and fuel feed ratio FR (or air excess number). Compressed air was introduced from the bottom of the reactor and precisely controlled to maintain stable fluidization and combustion. As dried and ground sludge powders blocked the feed, they were compressed as pellets (i.e., pressed into disks at 150 kN for 2 min) for feeding into the FBC. A pump was used at the end of the sampling line to ensure a negative pressure inside the bed thus an addition of gas flow from the feeding system.

The furnace was heated from ambient to the targeted temperature (800 or 900 °C) at 10 °C/min, and the temperature was kept stable during the combustion trial. The total (bottom air supply + gas addition from feeding) and bottom air was controlled at 16.4 and 9.0 L/min, respectively. The sample feeding rate was 1 g/min, residence time was 3 s, and feeding ratio (FR) of fuel was set at 6 for a complete combustion. For each trial, ~60 g of died pellet sample (3–5 mm in length) was manually fed into the combustor over an hour. After the furnace was cooled down, agglomerates were collected carefully by hand-picking and bottom ash was separated by sieving from the solid residues, as the agglomerates and bottom ashes had different colors and a bigger size, compared with that of sand particles.

Chemical and Microstructural Analysis. Common ash-forming elements include Al, Cl, Ca, Fe, K, Mg, Na, P, S, Si, and Ti.^{9,11,23} and their presence in sludge and bottom ash after combustion at 900 °C under oxidizing conditions was determined by X-ray fluorescence (XRF) spectrometry (Philips, PW2400, Netherlands). The samples were further ground in alpha-alumina mortar to make sure the particles possess enough affinity to form a self-supported disk for XRF analysis. Sample disks were made at 10 tons of ram load for 2 min and then put into the sample cell of a XRF machine

Table 2. Agglomeration Observations in Long-Time Lasting Combustion Trials

sample ID	trials	sand type	temp (°C)	agglomeration degree
S1	01	fresh	900	sand particles attached on bottom ash
S1	02	degraded	900	new agglomerated pieces formed
S1	03	fresh	800	no agglomerate formation
S2	01	fresh	900	no agglomerate formation
S2	02	degraded	900	new agglomerated pieces formed
S3	01	fresh	900	less sand particles attached on bottom ash
S3	02	degraded	900	sand particles attached on bottom ash
S4	01	fresh	900	less sand particles attached on bottom ash
S4	02	degraded	900	new agglomerated pieces formed
S4	03	degraded	800	no agglomerate formation

that automatically does a scanning and gives quantitative results over each found element.

The morphology and chemical composition of the agglomerates were studied by scanning electron microscopy (SEM; JEOL, JSM5310, Japan) equipped with an energy-dispersive X-ray spectrometer (EDX; Link ISIS300, Oxford, UK). The acceleration voltage for SEM was 10–15 keV, and the sample distance was 15 mm.²⁴ Agglomerates were vacuum impregnated with an epoxy resin (Struers Epofix, Denmark), cured for about 8 h, and polished to a finish of about 1 μm using diamond paste. A gold sputter coating was applied to make the specimens conductive. Micrographs were collected in the backscattered and secondary electrons modes.

The quantitative powder X-ray diffraction (XRD; Shimadzu 6000, Japan) measurement was performed for identification of crystalline compounds in bed material and agglomerated particles. Patterns were collected using a Siemens D5005 Bragg–Brentano diffractometer with 40 kV and 40 mA Cu Kα ($\lambda = 1.54 \text{ \AA}$) radiation and step-scanned in the 2θ range 10°–80° at intervals of 0.02° with a stepping time of 14 s leading to a total collection time of 13.6 h. The quantitative phase was analyzed using the fundamental parameter Rietveld procedure as implemented in TOPAS-R (Bruker DiffracPlus, version 2.1).

Results and Discussion

Agglomeration. To investigate the agglomeration phenomena, combustion tests of four sludge samples were purposely conducted under oxidizing conditions from 800 to 900 °C, using fresh or degraded sand as the bed material in a bench-scale FBC reactor. In 7 cases, a slight agglomeration occurred even though the ash fusion temperature was more than 1000 °C with the observations collected on the basis of 10 trials (Table 2). Most of the trials can be grouped into four categories, and illustrated as follows: (i) no agglomerate formation, e.g., S1-3, S2-1, and S4-3; (ii) a few sand particles attached on bottom ash, e.g., S3-1 and S4-1; (iii) lots of sand particles attached on bottom ash, e.g., S1-1 and S3-2; (iv) new agglomerates formed, e.g., S1-2, S2-2, and S4-2. The agglomeration tendency followed the sequence as $i < ii < iii < iv$. It can be easily found from Table 2 that as the temperature increased from 800 to 900 °C, more serious agglomerate was formed if comparing S1-2 with S1-3 and S4-2 with S4-3. On the other hand, the agglomerate was formed more easily when degraded sand was used as bed material rather than fresh sand. This might be because certain minerals had condensed onto the degraded sand from previous

(23) Theis, M.; Skrifvars, B. J.; Zevenhoven, M.; Hupa, M.; Tran, H. *Fuel* **2006**, *85*, 2002–2011.

(24) Ollila, H. J.; Daavitsainen, J. H. A.; Nuutinen, L. H.; Tiainen, M. S.; Virtanen, M. E.; Laitinen, R. S. *Energy Fuels* **2006**, *20*, 591–595.

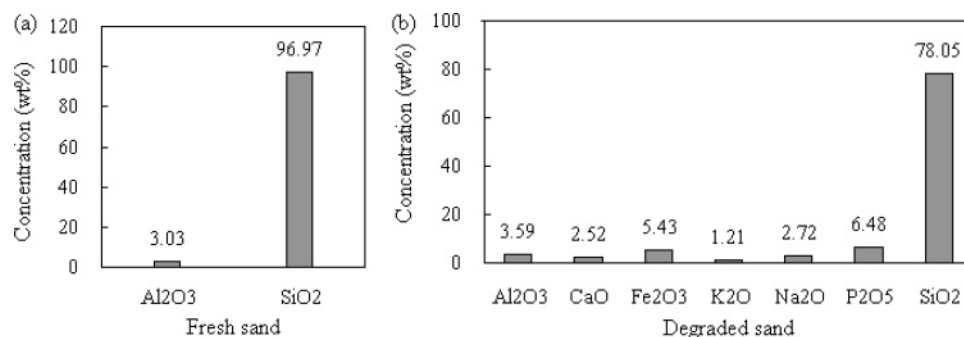


Figure 2. EDX analysis of the bed materials: (a) fresh sand and (b) degraded sand.

Table 3. XRF Results on Inorganic Matters of Ashing Sludge Samples (weight percent)

sample	SiO ₂	Al ₂ O ₃	CaO	MgO	K ₂ O	Na ₂ O	Fe ₂ O ₃	TiO ₂	P ₂ O ₅	SO ₃	Cl
S1	12.69	17.17	10.79	4.20	2.32	6.48	16.47	0.49	9.12	18.79	1.47
S2	20.44	21.54	8.22	3.34	2.65	5.83	14.19	0.47	9.24	12.91	1.16
S3	12.08	13.72	11.59	4.54	2.34	7.23	16.72	0.49	11.09	17.97	2.22
S4	7.76	16.18	11.03	4.57	2.72	8.00	18.42	0.55	11.83	16.73	2.20

Table 4. XRF Results on Inorganic Matters of Bottom Ash (weight percent)

sample	SiO ₂	Al ₂ O ₃	CaO	MgO	K ₂ O	Na ₂ O	Fe ₂ O ₃	TiO ₂	P ₂ O ₅	SO ₃	Cl
S1	37.63	18.04	9.66	3.68	2.23	3.05	17.04	0.49	8.10	0.00	0.09
S2	44.97	21.40	5.96	2.51	2.53	2.80	13.38	0.45	5.76	0.20	0.04
S3	39.82	14.38	8.16	3.90	2.07	4.01	16.16	0.47	10.74	0.25	0.05
S4	36.08	14.87	9.71	3.86	2.38	3.91	18.30	0.50	9.87	0.48	0.05

runs. Overall, only slight agglomerate formation was observed and no bed defluidization happened in all the testing trials conducted in this study.

The fresh sand and degraded sand were analyzed by SEM/EDX, and the results are shown in Figure 2. The main component is silica (~97% in fresh sand and ~78% in degraded sand) on the surface of sand particles. Besides SiO₂ and Al₂O₃, degraded sand also contained Ca, Fe, K, Na, and P. Nevertheless, most of those elements are associated with the formation of low melting point compounds, and therefore, they might accelerate the agglomerate formation in fluidized bed combustion. Another possibility is the formation of a thin coating layer by reaction among Si, Al, Ca, Fe, K, Na, and P, initiating agglomeration under certain critical conditions (e.g., temperature and coating thickness).^{19,20} Overall, to prevent bed agglomeration due to utilizing degraded sand, one option is to regularly change the bed material with the addition of fresh sand in practical applications.

Chemical Composition. Using XRF, the dominant species in the ashed sample (AS) were Si, Al, Ca, Fe, P, and S oxides while Si, Al, Ca, Fe, and P were the main components in the bottom ash (BA), shown in Tables 3 and 4. SiO₂ and SO₃ contents showed the greatest divergence with SiO₂ in the bottom ash much higher than that in the ashed sample, due to bed sand attachment onto the bottom ash. SO₃ in the bottom ash was much lower than in the ashed sample which resulted from substantial volatilization of sulfur during the combustion of sewage sludge in FBC at high temperature. Sodium and chlorine were subject to substantial evaporation at the higher temperature; therefore, their contents in the bottom ash were lower than that in the ashed sample. The sludge ashing samples were rich of alkali metals (K and Na), earth alkali metals (Ca and Mg), sulfur, iron, and phosphorus, which were mostly associated with the formation of low melting point eutectics.^{12,15,25}

Phase Assemblage. Fresh sand, degraded sand, and agglomerate particles were analyzed using XRD. The results are

Table 5. XRD Results of Agglomerate and Sand Sample

sample ID	SiO ₂ (low quartz) ^a	Fe ₂ O ₃ (hematite) ^a	unidentified phase
agglomerate	72%	28%	significant
fresh sand	100%	<i>b</i>	trace
degraded sand	100%	<i>b</i>	trace

^a Ignoring unidentified phases. ^b Below detection limit.

shown in Table 5. Both the fresh and degraded sand consisted primarily of quartz. Whereas, hematite (Fe₂O₃) and quartz (SiO₂) were the major crystalline components in sludge agglomerates accounting for 28 and 72 wt %, respectively, with Fe and Si bearing compounds possibly playing a major role in the formation of agglomerates. Minor unidentified crystalline phases were also present (Table 5). Only a few crystalline components were identified because other compounds in the agglomerates were either amorphous or the eutectics were too little to be detected; although in prior studies,²⁶ SiO₂, Fe₂O₃, CaCO₃, and CaSO₄ were found by XRD analysis of bed material agglomerates from Spanish sub-bituminous coal. The Si, Al, and Fe bearing compounds were found to be the main components in the ashing sludge samples (see Table 3); in considering the XRD results, they could suggest the main contribution of iron and silicon in bed agglomeration when sludge was combusted in FBC. In addition, alkali metals might also play an important role in agglomeration due to the formation of low-melting silicates, though their crystalline phase compounds were not found by XRD in the present study.

Microstructure and Microchemistry. The agglomerates formed from sludge combustion were provided for SEM/EDX analysis. The morphology of agglomerated particle was obtained by means of SEM scanning with second-scattered mode. A representative SEM image is shown in Figure 3. It vividly revealed the image of the agglomerate and the connection of bed material and ash particles.

(25) Dawson, M. R.; Brown, C. R. *Fuel* **1992**, *71*, 585–592.

(26) Steenari, B. M.; Lindqvist, O.; Langer, V. *Fuel* **1998**, *77*, 407–417.

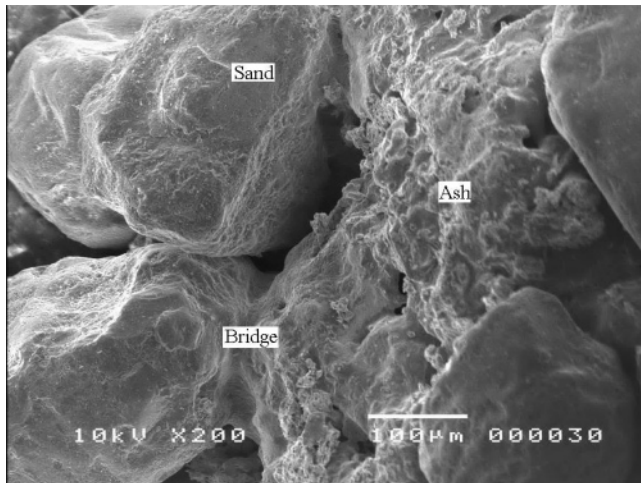


Figure 3. Morphology of agglomerates from sludge combustion by SEM.

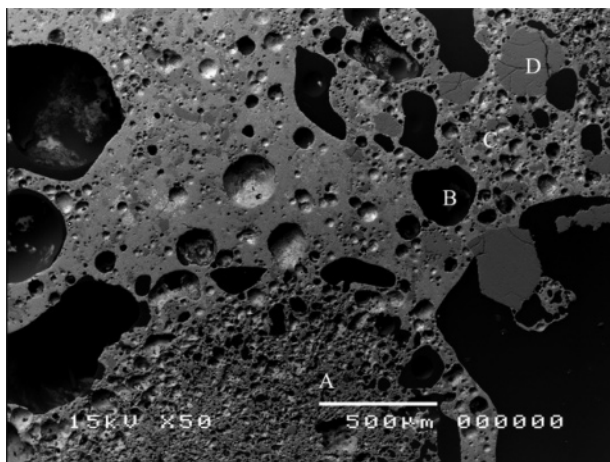


Figure 4. Overview of agglomerate sample by SEM/EDX analysis.

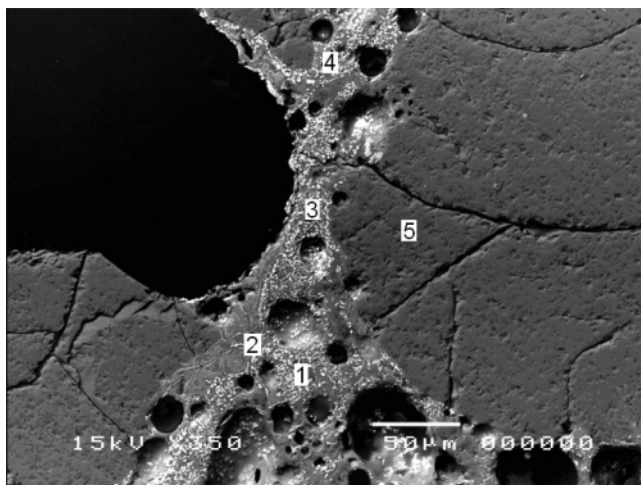


Figure 5. Bridge section of agglomerate sample for EDX analysis.

For a thorough SEM/EDX analysis, the granules of agglomerate formed from S2 combustion were treated with a series of pretreatment including impregnation, polishing, and coating, as mentioned previously. The SEM/EDX was operated in back-scattered mode, which helps to provide a better contrast of element distribution across the specimen surface. The results are presented in Figures 4–6. Figure 4 gives the overview of the S2 agglomerate's cross-section, including the bottom ash (A, the fiberlike area), the void space filled by epoxy (B, the

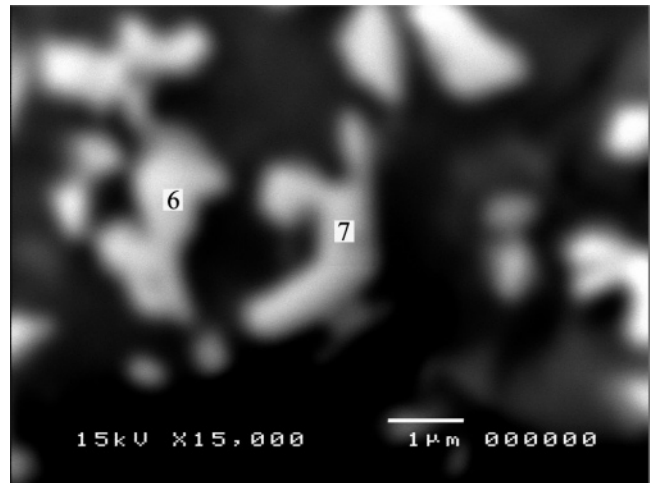


Figure 6. Selected white spot enlarged for further EDX analysis.

Table 6. SEM/EDX Analysis Results (weight percent)

area ID	SiO ₂	Al ₂ O ₃	CaO	MgO	K ₂ O	Na ₂ O	Fe ₂ O ₃	TiO ₂	P ₂ O ₅
1	25.26	14.74	3.66	4.04	3.42	5.47	26.42	0.67	16.32
2	35.54	10.25	6.85	5.34	2.7	4.02	10.69	-	24.62
3	27.88	13.55	1.75	4.44	2.98	4.55	29.32	0.77	14.76
4	30.17	17.54	2.57	2.17	3.79	6.87	22.53	0.51	13.85
5	100	a	a	a	a	a	a	a	a
6	17.73	11.01	1.39	4.57	2.17	2.64	47.13	2.23	11.12
7	15.12	10.13	1.26	5.05	1.82	3.45	49.93	1.78	11.45

^a Below detection limit.

jet black region), the agglomerate bridge (C, gray), and the bonded sand particle (D, darker patch). The close-up view of region D and the vicinity is presented in Figure 5 where different sample points (1, 2, 3, 4, and 5) were marked, and their chemical compositions were analyzed using EDX as shown in Table 6. Among them, point 5 in the deeper gray color zones represented sand particles while points 1, 2, 3, and 4 in lighter gray color zones represented the bridges in conjunction with sand particles, which formed due to certain low melting point components occurring in sludge combustion. The two groups of points were supposed to have different chemical compositions. In Figure 6, the sample point 3 from Figure 5 was enlarged to show the micro-inhomogeneity presented in bridge (light color) zones as white spots as a result of possibly certain heavy element enrichment.

The EDX quantitative results that match the five sampling points of Figure 5 and two white spots of Figure 6 are summarized in Table 6. It confirmed that the points (5) that fall on darker patches (sand particle zone) are pure sand (SiO₂) including only the elements of silicon and oxygen, and the contents of all other elements there are below the EDX detection limit. The cross section of agglomerates (points 1–4) shows a wealth of elements that may account for the forming of a bridge between sand particles due to their fusion property. Iron (Fe₂O₃) was found to be enriched in the bridges and presented almost at the same level of silicon (SiO₂) at ~20–30%. Other important elements found there include aluminum (Al) and phosphorus (P) at the level of 10–25%, followed by Ca, Mg, K, and Na at a level of 1–7%. Only a small amount of Ti (<1%) was found at the bridges. The microsized white spot (points 6 and 7) scattered across the ash continuum showed in Figure 6 was more enriched with Fe₂O₃ than SiO₂, with a level of the former at ~50% and that of the latter at ~15%, indicating possibly the major role of Fe in the formation of the agglomerated bridge. That is because the eutectics of hematite (Fe₂O₃) and quartz

(SiO₂) will give a melt phase at 900–1000 °C.²⁶ Results from FBC experiments in Table 6 showed the formation of agglomerates likely resulted from the sticky iron-silicate particles, for agglomerations were observed from most of the cases when the furnace temperature was set at 900 °C. This observation is in agreement with the XRD analysis as only Fe₂O₃ and SiO₂ were found in agglomerated samples with crystalline phase. Also, it was previously reported that the presence of iron in peat ash resulted in severe slagging and agglomeration as the possible interaction between ash and quartz bed sand to form iron aluminosilicates with low melting points.⁸

Comparing the four sampling points (1, 2, 3, and 4) at bridges, the location of point 2 is much closer to the sand particle representing the initial formation of the bridge. The composition of point 2 is different from that of the other three points, although they are all located at bridge zones. The concentrations of Si, P, Mg, and Ca at point 2 are obviously higher than those of points 1, 3, and 4, while concentrations of other elements (K, Na, Al, Fe) at point 2 are lower than those found at the other three point locations. This might imply the role of Si (from sand particles) and P, Mg, and Ca (from sludge) in initializing the formation of sticky surfaces of sand particles acting as a glue matter, followed by the formation of the agglomerate bridge contributed mostly by Fe, then by Al, K, and Na. For further confirmation, elements mapping is to be conducted in the future study.

In our previous work,⁵ the elements with high concentrations found at the bridge, which bond the sand particles, included only Si, Al, Fe, V, K and Na. A very low concentration of V was detected in the present sludge samples; thus, it will not be a concern of agglomerate formation in this study. But, several new elements (P, Ca, and Mg) were found to be associated with the agglomerate formation in sludge combustion, attributed most likely to the different chemical natures of the studied samples. The present result is consistent with the previous observations^{10,12} that Na, K, P, Mg, and Ca were the major elements in the bridge section by SEM/EDX.

According to the above analysis, the mechanism for forming agglomerates in sludge combustion might go to both coating-induced and melt-induced pathways. For the former, a coating layer enriched in Si, P, and Ca on the degraded sand particle (see Figure 2) may form a sticky surface and initiate the agglomeration, followed by a further development of the connection bridge due to the high existence of Fe, Al, K, and Na (Figure 2). Fresh sands should behave the same as degraded sands after being used for one trial, due to the vaporization and recondensation of those mentioned elements on sand particles. It was responsible for the adhesion of sand particles to bottom ash, as evidenced in Table 2 for the cases of S1-1 and S3-2. On the other hand, low-melting eutectics of iron-based silicates might be formed with subsequent viscous-flow sintering and agglomeration. In this study, melt-induced agglomeration seemed to be the dominating mechanism for those bed particles directly glued together, resulting from low melting point compounds, to form new pieces of agglomerates, as seen in the cases of S1-2, S2-2, and S4-2 in Table 2. Those low melting point compounds could be the sintering promoters. Experimentally, it is almost impossible to detect the speciation of these compounds due to the complexity of ash chemistry. Thermodynamic calculation on the predominant mineral species at desired combustion conditions can help to obtain a clearer understanding to the low melting point compounds.

Thermodynamic Calculation. The thermodynamic multiphase multicomponent equilibrium (TPCE) calculation was

Table 7. Major Species of Mineral Elements in Sludge Combustion under Oxidizing Conditions (Air Excess Ratio $\lambda = 1.2$)

element	major species and temperature range
Al	Al ₂ (SO ₄) ₃ (<600 °C), Al ₂ O ₃ (400–740 °C), Al ₂ O ₃ ·SiO ₂ (D) (>500 °C), Al ₂ SiO ₅ (>460 °C), AlPO ₄ (>640 °C), Ca ₂ Al ₂ SiO ₇ (>640 °C), CaAl ₂ Si ₃ O ₁₀ (OH) ₂ (<850 °C), and KAl(SO ₄) ₂ (<600 °C)
Ca	Ca ₂ Al ₂ SiO ₇ (>640 °C), CaAl ₂ Si ₃ O ₁₀ (OH) ₂ (<850 °C), and CaSO ₄ (<750 °C)
Fe	Fe ₂ (SO ₄) ₃ (<600 °C), Fe ₂ O ₃ (>400 °C), Fe ₃ O ₄ (>750 °C), FeO (>900 °C), FeSO ₄ (<700 °C), and MgFe ₂ O ₄ (>600 °C)
K	K ₂ SO ₄ (>720 °C), K ₂ SO ₄ ·2MgSO ₄ (<900 °C), K ₃ PO ₄ (>800 °C), KAl(SO ₄) ₂ (<600 °C), KCl(g) (>800 °C), KOH(g) (>1000 °C), and KPO ₃ (>750 °C)
Mg	Mg ₃ (PO ₄) ₂ (>700 °C), MgFe ₂ O ₄ (>600 °C), MgO (>680 °C), MgSiO ₃ (>760 °C), and MgSO ₄ (<900 °C)
Na	Na ₂ P ₂ O ₆ (>750 °C), Na ₂ SO ₄ (400–1200 °C), Na ₃ PO ₄ (>800 °C), NaAlSiO ₄ (>900 °C), NaCl(g) (>800 °C), and NaPO ₃ (>700 °C)
Si	Al ₂ O ₃ ·SiO ₂ (D) (>500 °C), Al ₂ SiO ₅ (>460 °C), CaAl ₂ Si ₃ O ₁₀ (OH) ₂ (<850 °C), MgSiO ₃ (>760 °C), NaAlSiO ₄ (>900 °C), and SiO ₂ (>750 °C)
Ti	TiO ₂ (400–1200 °C)

carried out using HSC software, based on the principle of minimizing the total Gibbs energy of a system. The method is based on well-established thermodynamic principles. It can provide comprehensive information about the system studied and give a first description of ash reactions in complex systems. However, the limitations of the method must be considered when interpreting results from thermodynamic analysis, as the equilibrium is based on the assumption of infinite reaction times and perfect mixing.

The input values of the HSC chemistry program were determined from sludge compositions. Sample S1 was selected as a representative. It was defined by its combustible C, H, N, S, and O contents, and its mineral elements including Si, Al, Ca, Mg, K, Na, Fe, Ti, P, S, and Cl. The molecular formula of sample S1 was normalized as CH_{2.298}O_{0.927}N_{0.079}S_{0.012} based on the composition of sludge as given in Table 1. The molar number for each mineral element input was calculated on the basis of ash composition as showed in Table 3. The considered temperature ranged from 400 to 1200 °C, and pressure was 1 atm. The air excess number (λ) was set as 1.2 for oxidizing conditions. The composition of air was assumed as 79% N₂ and 21% O₂. The introduction of the calculation method in detail can refer to our previous study.⁵

After computation, the main mineral species and their existing temperature range in the combustion system, which are thermodynamically favorable, are shown in Table 7. More attention should be paid to the elements which were found to be enriched in the agglomerates especially in the bridge section, including Si, Fe, P, Al, Ca, Mg, K, and Na. Their potential species as low melting point compounds, and their different presences at the desired operating conditions could be figured out from the computation.

According to previous literature and handbooks,^{27,28} the predicted agglomeration promoters with low melting point in this study are Al₂(SO₄)₃ (770 °C), Na₂SO₄ (884 °C), Fe₂(SO₄)₃ (480 °C), K₂SO₄ (1069 °C), FeSO₄ (661 °C), KPO₃ (450 °C), NaPO₃ (627 °C), and the eutectics of Fe₂O₃ and SiO₂ (900–1000 °C). The melting point is indicated in the parentheses. In the thermodynamic point-of-view, most of these species would be formed at lower temperature and might melt to form a liquid-

(27) Vuthaluru, H. B.; Zhang, D. k. *Fuel Process. Technol.* **2001**, *69*, 13–27.

(28) Perry, R. H.; Green, D. W. *Perry's Chemical Engineers' Handbook*, 7th ed; McGraw-Hill: New York, 1997; p 2581.

phase surface, which makes the ash sticky and facilitates the particles attaching together and resulting in large agglomerate particles. Nevertheless, a very small amount of sulfur was found in the bottom ash, agglomerates, and degraded sands (see Table 4, Table 6, and Figure 3b, respectively), although lots of sulfur existed in ashing sludge samples (Table 3). The majority of sulfur was emitted into the gas phase at high temperature as predicted in the calculation. Therefore, sulfates might not be enriched in bed materials to serve as the agglomeration promoters, as predicted. On the other hand, the alkali phosphate (KPO_3 and NaPO_3) and the eutectics of Fe_2O_3 and SiO_2 were most likely the main agglomeration promoters with low melting points, as predicted from thermodynamic calculation and evidenced in bed materials identification—a significant amount of K, Na, P, Fe, and Si were found in the bottom ash, agglomerated bridge, and degraded sands. Also, hematite (Fe_2O_3) and quartz (SiO_2) were detected by XRD in the agglomerate particles.

The effect of temperature, pressure, air excess number, and mixing ratio of sludge samples on the formation of low melting point compounds will be considered further in thermodynamic simulation.

Conclusions

The agglomeration characteristics in sludge combustion were investigated in a bench-scale fluidized bed combustor. Slight agglomeration was observed in 7 out of 10 cases of sludge combustion. Agglomeration invariably became more severe at higher temperatures with degraded sand as bed material compared to fresh sand. Detail analysis indicated that, besides Al and Si, several elements (Ca, Fe, K, Na, and P) that are believed to be associated with the formation of low melting point compounds were enriched in degraded sands.

Only Fe_2O_3 and SiO_2 were found to be the major crystalline components in agglomerates while the amorphous phase cannot be identified by XRD. SEM/EDX analysis confirmed that Fe and Si were enriched in the bridge connecting sand particles.

The agglomeration process was revealed by a series of morphology images of ash–sand particle agglomerates, suggesting the potential role of Si (from sand particles) and P, Mg, and Ca (from sludge) in initializing the formation of the sticky surface of sand particles acting as a glue matter, followed by the formation of an agglomerate bridge contributed most likely by Fe, then by Al, K, and Na.

The possible mechanisms of bed agglomeration in sludge combustion were attributed to both melt-induced and coating-induced pathways. First, low-melting eutectics of iron silicates might be formed with subsequent viscous-flow sintering and agglomeration, responsible for bed particles directly glued together by a separated ash-derived melt phase. Second, a coating layer enriched in Si, P, and Ca on the degraded sand particle may form a sticky surface and initiate the agglomeration, responsible for the adhesion of sand particles to bottom ashes.

The TPCE calculation can be used as a helpful tool to better understand the ash-forming behavior and to predict the bed agglomeration during sludge combustion in FBC. The predicted bed agglomeration promoters included $\text{Al}_2(\text{SO}_4)_3$, Na_2SO_4 , $\text{Fe}_2(\text{SO}_4)_3$, K_2SO_4 , FeSO_4 , KPO_3 , NaPO_3 , and eutectics of Fe_2O_3 and SiO_2 under oxidizing conditions, which are thermodynamically favorable species existing in the complex combustion system. After taking into account both experimental and computational results, it is believed that only alkali phosphates (KPO_3 and NaPO_3) and the eutectics of Fe_2O_3 and SiO_2 might play the most important role in bed agglomeration, by forming low melting point compounds, in the course of sludge combustion.

Acknowledgment. This work is part of the project “Co-control of Pollutants during Solid Fuel Utilization”, supported by the Programme of Introducing Talents of Discipline to Universities (project B06019), China. The authors would like to acknowledge Ms. Joon Hua Heng at the School of Materials Science and Engineering in Nanyang Technological University for her help in SEM/EDX and XRD analysis.

EF070004Q